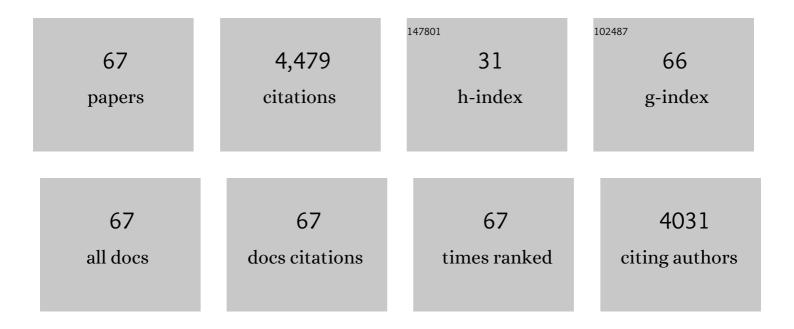
Jianping Zou

List of Publications by Year in descending order

Source: https://exaly.com/author-pdf/4112497/publications.pdf Version: 2024-02-01



IMNDING ZOU

#	Article	IF	CITATIONS
1	Lattice expansion boosting photocatalytic degradation performance of CuCo2S4 with an inherent dipole moment. Chinese Chemical Letters, 2023, 34, 107468.	9.0	26
2	Halogenated benzothiadiazole-based conjugated polymers as efficient photocatalysts for dye degradation and oxidative coupling of benzylamines. Chinese Chemical Letters, 2022, 33, 2736-2740.	9.0	11
3	Semi-chemical interaction between graphitic carbon nitride and Pt for boosting photocatalytic hydrogen evolution. Chinese Chemical Letters, 2022, 33, 3061-3064.	9.0	12
4	Shifts of surface-bound •OH to homogeneous •OH in BDD electrochemical system via UV irradiation for enhanced degradation of hydrophilic aromatic compounds. Chemosphere, 2022, 291, 132817.	8.2	20
5	Mineralization of cyanides via a novel Electro-Fenton system generating •OH and •O2â^. Water Research, 2022, 209, 117890.	11.3	51
6	Selective regulation of peroxydisulfate-to-hydroxyl radical for efficient in-situ chemical oxidation over Fe-based metal-organic frameworks under visible light. Journal of Catalysis, 2022, 406, 1-8.	6.2	13
7	Detection and Removal of Mercury Ions in Water by a Covalent Organic Framework Rich in Sulfur and Nitrogen. ACS Applied Polymer Materials, 2022, 4, 849-858.	4.4	22
8	A new strategy for the fabrication of covalent organic framework-metal-organic framework hybrids via in-situ functionalization of ligands for improved hydrogen evolution reaction activity. Chinese Journal of Catalysis, 2022, 43, 811-819.	14.0	13
9	High-throughput lateral and basal interface in CeO2@Ti3C2TX: Reverse and synergistic migration of carrier for enhanced photocatalytic CO2 reduction. Journal of Colloid and Interface Science, 2022, 615, 716-724.	9.4	11
10	New insights on the role of NaCl electrolyte for degradation of organic pollutants in the system of electrocatalysis coupled with advanced oxidation processes. Journal of Environmental Chemical Engineering, 2022, 10, 107414.	6.7	19
11	Degradation of pesticide wastewater with simultaneous resource recovery via ozonation coupled with anaerobic biochemical technology. Chemosphere, 2022, 300, 134520.	8.2	9
12	lsotypic heterojunction based on Fe-doped and terephthalaldehyde-modified carbon nitride for improving photocatalytic degradation with simultaneous hydrogen production. Chinese Chemical Letters, 2021, 32, 2782-2786.	9.0	21
13	New Insights into the Degradation of Atrazine by Ultraviolet-Based Techniques. ACS ES&T Water, 2021, 1, 958-968.	4.6	5
14	Transformation of Atrazine to Hydroxyatrazine with Alkali-H ₂ O ₂ Treatment: An Efficient Dechlorination Strategy under Alkaline Conditions. ACS ES&T Water, 2021, 1, 1868-1877.	4.6	9
15	Carbon Nitride Supported High‣oading Fe Singleâ€Atom Catalyst for Activation of Peroxymonosulfate to Generate ¹ O ₂ with 100 % Selectivity. Angewandte Chemie - International Edition, 2021, 60, 21751-21755.	13.8	521
16	Selective oxidation of diclofenac sodium with different electronegative moieties via coexisting SO4â^' and OH. Science of the Total Environment, 2021, 782, 146857.	8.0	19
17	Carbon Nitride Supported High‣oading Fe Singleâ€Atom Catalyst for Activation of Peroxymonosulfate to Generate 1 O 2 with 100 % Selectivity. Angewandte Chemie, 2021, 133, 21919-21923.	2.0	18
18	Oxygen migration triggering molybdenum exposure in oxygen vacancy-rich ultra-thin Bi2MoO6 nanoflakes: Dual binding sites governing selective CO2 reduction into liquid hydrocarbons. Journal of Energy Chemistry, 2021, 61, 281-289.	12.9	40

JIANPING ZOU

#	Article	IF	CITATIONS
19	Bioavailability quantification and uptake mechanisms of pyrene associated with different-sized microplastics to Daphnia magna. Science of the Total Environment, 2021, 797, 149201.	8.0	16
20	Functional groups to modify g-C3N4 for improved photocatalytic activity of hydrogen evolution from water splitting. Chinese Chemical Letters, 2020, 31, 1648-1653.	9.0	99
21	Highly durable isotypic heterojunction generated by covalent cross-linking with organic linkers for improving visible-light-driven photocatalytic performance. Applied Catalysis B: Environmental, 2020, 260, 118182.	20.2	20
22	WS2 quantum dots seeding in Bi2S3 nanotubes: A novel Vis-NIR light sensitive photocatalyst with low-resistance junction interface for CO2 reduction. Chemical Engineering Journal, 2020, 389, 123430.	12.7	82
23	Highly efficient charge transfer in CdS-covalent organic framework nanocomposites for stable photocatalytic hydrogen evolution under visible light. Science Bulletin, 2020, 65, 113-122.	9.0	115
24	Degradation of 4-nitrophenol by electrocatalysis and advanced oxidation processes using Co3O4@C anode coupled with simultaneous CO2 reduction via SnO2/CC cathode. Chinese Chemical Letters, 2020, 31, 1961-1965.	9.0	118
25	Silver Single Atom in Carbon Nitride Catalyst for Highly Efficient Photocatalytic Hydrogen Evolution. Angewandte Chemie, 2020, 132, 23312-23316.	2.0	46
26	Efficient Capture of Volatile Iodine by Thiophene-Containing Porous Organic Polymers. ACS Applied Polymer Materials, 2020, 2, 5121-5128.	4.4	36
27	Unveiling localized Pt–P–N bonding states constructed on covalent triazine-based frameworks for boosting photocatalytic hydrogen evolution. Journal of Materials Chemistry A, 2020, 8, 25425-25430.	10.3	32
28	Silver Single Atom in Carbon Nitride Catalyst for Highly Efficient Photocatalytic Hydrogen Evolution. Angewandte Chemie - International Edition, 2020, 59, 23112-23116.	13.8	270
29	Bi ₂ MoO ₆ Quantum Dots In Situ Grown on Reduced Graphene Oxide Layers: A Novel Electron-Rich Interface for Efficient CO ₂ Reduction. ACS Applied Materials & Interfaces, 2020, 12, 25861-25874.	8.0	46
30	Great Divergence Exists in Chinese Provincial Trade-Related CO ₂ Emission Accounts. Environmental Science & Technology, 2020, 54, 8527-8538.	10.0	16
31	Chlorine-mediated photocatalytic hydrogen production based on triazine covalent organic framework. Applied Catalysis B: Environmental, 2020, 272, 118989.	20.2	44
32	High selective reduction of nitrate into nitrogen by novel Fe-Cu/D407 composite with excellent stability and activity. Environmental Pollution, 2019, 252, 888-896.	7.5	25
33	Dechlorination-Hydroxylation of Atrazine to Hydroxyatrazine with Thiosulfate: A Detoxification Strategy in Seconds. Environmental Science & amp; Technology, 2019, 53, 3208-3216.	10.0	41
34	A general strategy <i>via</i> chemically covalent combination for constructing heterostructured catalysts with enhanced photocatalytic hydrogen evolution. Chemical Communications, 2019, 55, 4150-4153.	4.1	45
35	Design and syntheses of MOF/COF hybrid materials via postsynthetic covalent modification: An efficient strategy to boost the visible-light-driven photocatalytic performance. Applied Catalysis B: Environmental, 2019, 243, 621-628.	20.2	253
36	Electrochemical oxidation and advanced oxidation processes using a 3D hexagonal Co3O4 array anode for 4-nitrophenol decomposition coupled with simultaneous CO2 conversion to liquid fuels via a flower-like CuO cathode. Water Research, 2019, 150, 330-339.	11.3	147

JIANPING ZOU

#	Article	IF	CITATIONS
37	Photoelectrochemical Degradation of Organic Pollutants Using BiOBr Anode Coupled with Simultaneous CO ₂ Reduction to Liquid Fuels via CuO Cathode. ACS Sustainable Chemistry and Engineering, 2019, 7, 1250-1259.	6.7	43
38	A new strategy for triggering photocatalytic activity of Cytrochrome P450 by coupling of semiconductors. Chemical Engineering Journal, 2019, 358, 58-66.	12.7	12
39	Photocatalytic degradation of organic pollutants coupled with simultaneous photocatalytic H2 evolution over graphene quantum dots/Mn-N-TiO2/g-C3N4 composite catalysts: Performance and mechanism. Applied Catalysis B: Environmental, 2018, 227, 312-321.	20.2	246
40	Simultaneous photoreduction of Uranium(VI) and photooxidation of Arsenic(III) in aqueous solution over g-C3N4/TiO2 heterostructured catalysts under simulated sunlight irradiation. Applied Catalysis B: Environmental, 2018, 228, 29-38.	20.2	260
41	Hierarchical CeO2/Bi2MoO6 heterostructured nanocomposites for photoreduction of CO2 into hydrocarbons under visible light irradiation. Applied Surface Science, 2018, 434, 481-491.	6.1	105
42	Synthesis and characterizations of metal-free Semiconductor/MOFs with good stability and high photocatalytic activity for H2 evolution: A novel Z-Scheme heterostructured photocatalyst formed by covalent bonds. Applied Catalysis B: Environmental, 2018, 220, 607-614.	20.2	209
43	Mechanism investigation of anoxic Cr(VI) removal by nano zero-valent iron based on XPS analysis in time scale. Chemical Engineering Journal, 2018, 335, 945-953.	12.7	174
44	Size-controlled synthesis of CdS nanoparticles confined on covalent triazine-based frameworks for durable photocatalytic hydrogen evolution under visible light. Nanoscale, 2018, 10, 19509-19516.	5.6	108
45	Photodegradation of Organic Pollutants Coupled with Simultaneous Photocatalytic Evolution of Hydrogen Using Quantum-Dot-Modified g-C ₃ N ₄ Catalysts under Visible-Light Irradiation. ACS Sustainable Chemistry and Engineering, 2018, 6, 12695-12705.	6.7	102
46	Enhanced photocatalytic reduction of CO2 into alcohols on Z-scheme Ag/Ag3PO4/CeO2 driven by visible light. Materials Letters, 2018, 232, 36-39.	2.6	38
47	Coupling of photodegradation of RhB with photoreduction of CO 2 over rGO/SrTi 0.95 Fe 0.05 O 3â~ Î′ catalyst: A strategy for one-pot conversion of organic pollutants to methanol and ethanol. Journal of Catalysis, 2017, 349, 218-225.	6.2	74
48	Three-Dimensional Reduced Graphene Oxide Coupled with Mn ₃ O ₄ for Highly Efficient Removal of Sb(III) and Sb(V) from Water. ACS Applied Materials & Interfaces, 2016, 8, 18140-18149.	8.0	120
49	Synthesis and efficient visible light photocatalytic H2 evolution of a metal-free g-C3N4/graphene quantum dots hybrid photocatalyst. Applied Catalysis B: Environmental, 2016, 193, 103-109.	20.2	218
50	A Strategy for One-Pot Conversion of Organic Pollutants into Useful Hydrocarbons through Coupling Photodegradation of MB with Photoreduction of CO ₂ . ACS Catalysis, 2016, 6, 6861-6867.	11.2	128
51	Fabrication of novel heterostructured few layered WS2-Bi2WO6/Bi3.84W0.16O6.24 composites with enhanced photocatalytic performance. Applied Catalysis B: Environmental, 2015, 179, 220-228.	20.2	78
52	High-performance heterostructured CdS/Ba1â^'xSrxTiO3 system with unique synergism for photocatalytic H2 evolution. Applied Catalysis A: General, 2015, 493, 58-67.	4.3	22
53	Highly efficient and stable hydrogen evolution from water with CdS as photosensitizer—A noble-metal-free system. Applied Catalysis B: Environmental, 2014, 150-151, 466-471.	20.2	28
54	A new CdS/Bi1â^'In TaO4 heterostructured photocatalyst containing solid solutions for H2 evolution from water splitting. International Journal of Hydrogen Energy, 2014, 39, 13105-13113.	7.1	8

JIANPING ZOU

#	Article	IF	CITATIONS
55	Effect of ultrasound on sodium arsenate induction time and crystallization property during solution crystallization processes. Acoustical Physics, 2014, 60, 356-360.	1.0	8
56	Graphene oxide as structure-directing and morphology-controlling agent for the syntheses of heterostructured graphene-Bi2MoO6/Bi3.64Mo0.36O6.55 composites with high photocatalytic activity. Applied Catalysis B: Environmental, 2014, 156-157, 447-455.	20.2	63
57	A novel (4,6)-connected 3D metal-organic framework based on chelidamic acid: Synthesis, crystal structure and photoluminescence. Inorganic Chemistry Communication, 2013, 35, 326-329.	3.9	3
58	Synthesis, Band and Crystal Structures, and Optical Properties of the Ternary Compound Mg ₂ Te ₃ O ₈ . Zeitschrift Fur Anorganische Und Allgemeine Chemie, 2013, 639, 31-34.	1.2	12
59	Syntheses, crystal structures, and optical properties of a series of transition metal coordination polymers with chelidamic acid and 4,4′-bipyridine. Journal of Coordination Chemistry, 2012, 65, 2877-2892.	2.2	12
60	Synthesis, crystal and band structures, and optical properties of a new framework mercury pnictides: [Hg4As2](InBr3.5As0.5) with tridymite topology. Journal of Alloys and Compounds, 2011, 509, 221-225.	5.5	20
61	Syntheses, Structures and Optical Properties of a Series of Lanthanide Complexes with Chelidamic Acid and 4,4′-Bipyridyl. Journal of Chemical Crystallography, 2011, 41, 1820-1833.	1.1	9
62	Two heterometal–organic coordination polymers with chelidamic acid: Syntheses, structures and optical properties. Inorganica Chimica Acta, 2011, 373, 243-248.	2.4	7
63	Syntheses, crystal structures, and magnetic and luminescent properties of a series of lanthanide coordination polymers with chelidamic acid ligand. Polyhedron, 2010, 29, 2674-2679.	2.2	21
64	3-D Hydrogen-bonded networks of metal complexes with chelidamic acid and 1,10-phenanthroline: syntheses, structures, and optical properties. Journal of Coordination Chemistry, 2010, 63, 3576-3588.	2.2	7
65	Syntheses, structures, and optical properties of two cadmium complexes with chelidamic acid. Journal of Coordination Chemistry, 2010, 63, 56-66.	2.2	13
66	A 1-D chain praseodymium complex with chelidamic acid: synthesis, structure, and optical properties. Journal of Coordination Chemistry, 2009, 62, 3324-3331.	2.2	17
67	Synthesis, crystal and band structures, and optical and magnetic properties of a 1D copper coordination polymer with chelidamic acid ligand. Inorganica Chimica Acta, 2009, 362, 4843-4848.	2.4	23